

## Size dependence of exciton-exciton scattering in semiconductor quantum wires

W. Braun, M. Bayer, and A. Forchel

*Technische Physik, Universität Würzburg, Am Hubland, D-97074 Würzburg, Germany*

O. M. Schmitt, L. Bányai, and H. Haug

*Institut für Theoretische Physik, J. W. Goethe Universität Frankfurt, Robert-Mayer-Strasse 8, D-60054 Frankfurt a.M., Germany*

A. I. Filin

*Institute of Solid State Physics, Russian Academy of Sciences, 142432 Chernogolovka, Russia*

(Received 4 December 1997)

The exciton dephasing kinetics due to exciton-exciton scattering is studied in  $\text{In}_{0.135}\text{Ga}_{0.865}\text{As}/\text{GaAs}$  quantum wires both experimentally and theoretically as a function of the wire width. By degenerate four-wave mixing studies, we observe a strong increase of the exciton-density-dependent dephasing rate for decreasing wire widths between 85 nm and 29 nm. This surprising result is explained quantitatively within a multisubband model in terms of the increase of the exchange part of the exciton-exciton interaction with increasing confinement. [S0163-1829(98)01419-2]

It is generally assumed that the relaxation and dephasing kinetics of excited carriers slows down with increasing quantum confinement due to the reduction of phase space for the scattering processes. Benisty, Sotomayor-Torrès, and Weisbuch<sup>1</sup> argued, e.g., that in quantum dots the capture and relaxation kinetics of the carriers by phonon emission becomes so slow that it would prevent the realization of efficient quantum-dot lasers. Similarly, in strongly confined quantum wires (QWW's) enhanced carrier mobilities<sup>2</sup> are expected, when the energy splitting between the subbands exceeds the LO-phonon energy. However, little is known about the effects of increasing confinement on Coulombic scattering kinetics, except that it may partly overcome the bottlenecks by phonon relaxation.<sup>3</sup> The Coulomb interaction increases, as can be observed in larger exciton binding energies in QWW's.<sup>4-8</sup> However, the phase space is reduced; thus it remains an open question which effect will dominate.

We will demonstrate experimentally and theoretically for the example of the dephasing of coherent excitons ( $X$ 's), by scattering with incoherent  $X$ 's in QWW's, that there is no monotonic decrease of the scattering rates for increasing confinement. On the contrary, our results show that the dephasing rates due to Coulomb scattering increase strongly with decreasing wire width  $L_x$ .

While for low excitation intensities the  $X$  relaxation kinetics is governed by phonon and disorder scattering,<sup>9</sup>  $X$ - $X$  scattering dominates in an intermediate excitation regime. Up to now, there is no systematic experimental investigation for the changes of the  $X$  scattering in QWW's compared to systems of higher dimensionality. Oestreich *et al.*<sup>10</sup> found hints of a reduced scattering in 60-nm-wide  $\text{GaAs}/\text{Al}_{0.30}\text{Ga}_{0.70}\text{As}$  QWW's by using time-resolved photoluminescence spectroscopy, which they attributed to the reduced phase space of one-dimensional  $X$ 's. In contrast, Mayer *et al.*<sup>11</sup> found an enhanced scattering in 60-nm-wide QWW's by degenerate four-wave mixing studies. In both studies, the degree of confinement has not been varied, which did not allow a detailed study of the influence of the wire confine-

ment on the relaxation kinetics. Theoretically, to the best of our knowledge, no detailed model for  $X$ - $X$  scattering kinetics in QWW's has been developed.

We have investigated the dephasing of coherent  $X$ 's due to scattering with incoherent  $X$ 's. We find a strong enhancement of the  $X$ - $X$  scattering in wires with widths below 50 nm, which is in excellent agreement with the presented microscopic theory of the  $X$  dephasing kinetics. The comparison of the measurements with this theory reveals that the increased scattering rates are due to an increase of the exchange part of the  $X$ - $X$  interaction with decreasing QWW width.

The present experiments have been performed on free-standing  $\text{In}_x\text{Ga}_{1-x}\text{As}/\text{GaAs}$  QWW's with a width  $L_x$  ranging from 85 nm down to 29 nm. These structures were fabricated by electron-beam lithography and reactive dry etching from a multiple quantum well, consisting of 20  $\text{In}_{0.135}\text{Ga}_{0.865}\text{As}$  wells each with a thickness of 3 nm.<sup>12</sup> The lateral size of the QWW's was determined directly by high-resolution scanning electron micrographs. For comparison, we also investigated a quasi-two-dimensional reference.

Figure 1 shows photoluminescence (PL) and photoluminescence excitation (PLE) spectra of QWW's with varying width. For simplicity, only the spectral region around the ground-state heavy hole  $X$  is shown. When going from 85-nm- to 43-nm-wide QWW's, both PL and PLE lines of the  $X$  ground state are slightly redshifted due to strain release introduced by the lateral patterning. For small QWW's, a blueshift is observed due to the lateral quantization of the  $X$  wave function. The PL as well as PLE lines are only weakly broadened as the wire width is decreased, indicating a high sample quality. The full width at half maximum of the PL line increases from 2.8 meV for the 85-nm-wide QWW's, to 3.7 meV for the 29-nm-wide ones. The Stokes shift between the maxima of the PL and PLE lines, which is due to  $X$  localization effects, is nearly wire width independent, with a value of about 1.2 meV. In this type of QWW's, we have previously found a pronounced increase of the  $X$  binding

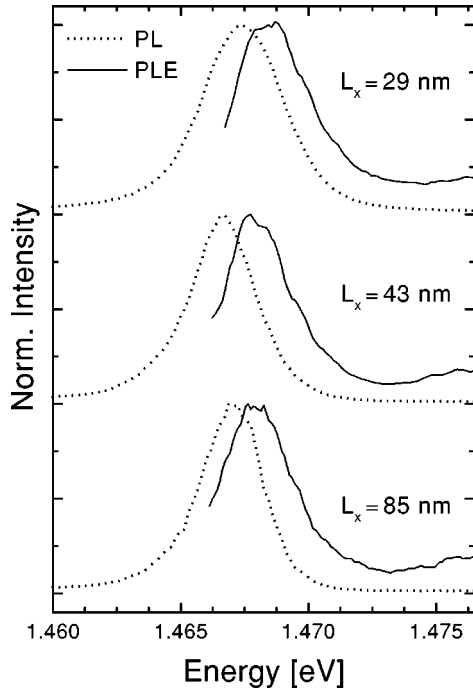


FIG. 1. Photoluminescence (dotted lines) and photoluminescence excitation spectra (solid lines) of three typical QWW's.

energy<sup>12</sup> for wire widths below about 50 nm due to the enhancement of the direct Coulomb interaction by the lateral quantization of the  $X$  wave function.

The  $X$ - $X$  scattering in these QWW's has been studied experimentally, using the technique of degenerate, time-integrated four-wave mixing (DFWM). We used a standard two-pulse self-diffraction configuration,<sup>13</sup> where two collinearly polarized pulses ( $\mathbf{k}_1, \mathbf{k}_2$ ) are focused upon the sample with a variable time delay  $\tau$  between them. The evolution of the signal in the direction  $2\mathbf{k}_2 - \mathbf{k}_1$  with the delay time  $\tau$  allows a direct measure of the phase coherence time  $T_2$ ,<sup>14</sup> which is connected with the homogeneous linewidth by  $\Gamma = 2\hbar/T_2$ .

To measure the homogeneous linewidth of the heavy-hole (hh) ground state  $X$  and to avoid the excitation of energetically higher-lying states, the pulses of a 70-fs titanium-sapphire laser were spectrally compressed to a width of about 6 meV, using a grating and a slit. The energy of the laser was tuned to a value slightly below the hh- $X$  resonance for each wire width individually. The time-integrated intensity of the DFWM pulses was  $0.8 \text{ kW/cm}^{-2}$ , resulting in an  $X$  density below  $3 \times 10^9 \text{ cm}^{-2}$ . All measurements were carried out at a temperature of 5 K.

From the decay of the DFWM signal, the phase-coherence time  $T_2$  has been determined as a function of the density of an incoherent  $X$  population, which has been excited by a prepulse of variable intensity hitting the sample 40 ps before the DFWM pulses, as shown schematically in Fig. 2. The  $X$  density generated by this pulse was determined from absorption spectra of the prepulse.<sup>15</sup>

Figure 3 shows the evolution of the DFWM signal versus delay time  $\tau$  for two different wire sizes, namely, for 85-nm-wide, quasi-two-dimensional wires (upper part) and for 29-nm-wide QWW's (lower part). From top to bottom the intensity of the prepulse has been increased. The estimated  $X$

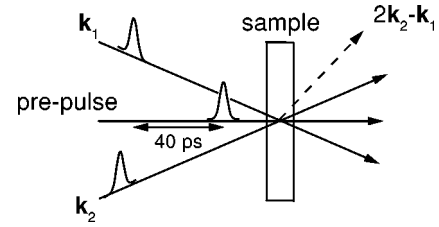


FIG. 2. Schematics of the four-wave mixing experiment. The prepulse generates an incoherent  $X$  population of varying density. The DFWM signal is detected in the direction  $2\mathbf{k}_2 - \mathbf{k}_1$ .

density ranges between  $2.9 \times 10^9 \text{ cm}^{-2}$  and  $2.3 \times 10^{10} \text{ cm}^{-2}$ , respectively, for the 85-nm-wide QWW's and between  $1.0 \times 10^9$  and  $4.7 \times 10^9 \text{ cm}^{-2}$  for the 29-nm-wide ones, as denoted in Fig. 3. From the semilogarithmic representation of the DFWM signal, the exponential decay of the coherent polarization with the delay time  $\tau$  is seen. The origin of the superimposed quantum beats will be discussed elsewhere. With increasing intensity of the prepulse, the dephasing of the  $X$ 's becomes faster due to the influence of  $X$ - $X$  scattering. In addition, the dephasing rate clearly increases with decreasing wire width, even for comparable low  $X$  densities.

From the slope of the decay curves  $\tau_S$ , we determine the phase relaxation time by  $T_2 = 4\tau_S$ , assuming that the transitions are mainly inhomogeneously broadened.<sup>14</sup> Figure 4 shows the homogeneous linewidths for 85-nm- and 29-nm-wide wires as functions of the  $X$  density  $n_X$ . In both cases,  $\Gamma$  depends linearly on the  $X$  density, as observed previously for quantum wells.<sup>16,17</sup> The  $X$  density dependence of the homogeneous linewidth is thus given by

$$\Gamma(n_X) = \Gamma_0 + \gamma_{XX} n_X. \quad (1)$$

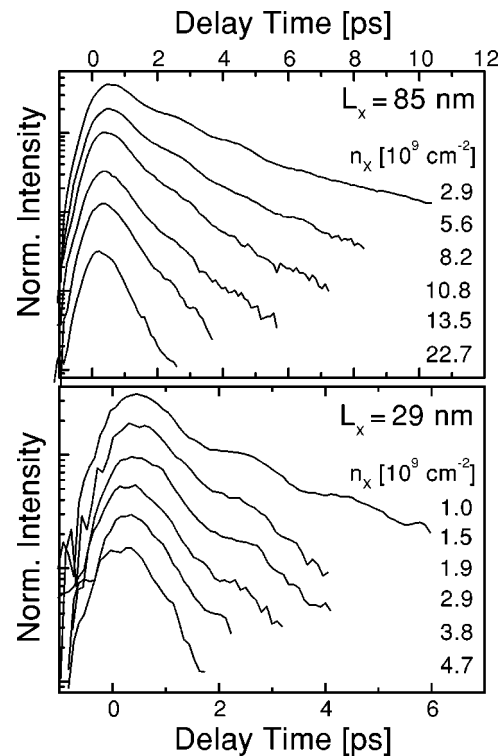


FIG. 3. Normalized DFWM signal for two QWW's with lateral sizes of 85 nm (upper part) and 29 nm (lower part), respectively.

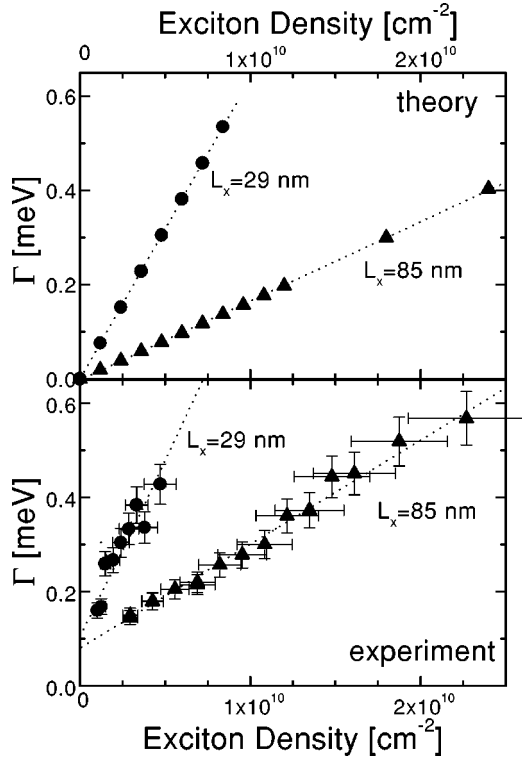


FIG. 4. Dependence of the homogeneous linewidth  $\Gamma$  on the  $X$  density for 85-nm- and 29-nm-wide QWW's. The dotted lines give linear fits to the data. The upper part of the figure presents the theoretical results.

Here  $\Gamma_0$  denotes the contribution which is not determined by  $X$ - $X$  scattering.  $\Gamma_0$  increases with decreasing wire width, which most probably is caused by residual scattering of  $X$ 's at wire-width fluctuations.

On the other hand, the slope  $\gamma_{XX}$  of  $\Gamma(n_X)$  depends strongly on the wire width  $L_x$ . In the smallest wires,  $\Gamma(n_X)$  increases significantly more strongly with  $n_X$  than in wide structures.  $\gamma_{XX}$  gives the strength of the  $X$ - $X$  scattering. This result therefore demonstrates a strongly enhanced  $X$ - $X$  scattering in small QWW's.

Both findings, the linear dependence of  $\Gamma$  on the  $X$  density and the wire-width dependence of  $\gamma_{XX}$ , are in very good agreement with results of detailed numerical calculations, as shown in the upper part of Fig. 4. For these calculations we have developed a microscopic model of the  $X$  kinetics in QWW's with widths  $L_x$  larger than the exciton Bohr radius  $a_B$ .  $\lambda = a_B/L_x < 1$  is used as an expansion parameter in this model. In this limit, mainly the center-of-mass motion of the  $X$ 's is quantized by the lateral confinement, while the relative motion is less affected. The  $X$  wave function can therefore be written as

$$\psi_{N,K}(\mathbf{r}_e, \mathbf{r}_h) = \sqrt{\frac{2}{L_x L_y}} \exp(iKR_y) \sin\left(\frac{N\pi R_x}{L_x}\right) \psi_{1s}^{2D}(\mathbf{r}), \quad (2)$$

where  $\mathbf{R}$  and  $\mathbf{r} = \mathbf{r}_e - \mathbf{r}_h$  describe the  $X$  center-of-mass and relative coordinates, respectively.  $K$  is the center-of-mass momentum of the  $X$  along the wire axis  $y$ , and  $N$  is the quantum number of the lateral  $X$  center-of-mass subbands

with a spacing between first and second subband of about 0.5 meV to 4 meV for the considered wires.  $\psi_{1s}^{2D}$  describes the relative two-dimensional electron-hole motion. The Hamiltonian of the interacting  $X$ 's with  $\nu = N, K$  in the boson approximation is given by

$$H = \sum_{\nu} \epsilon_{\nu} b_{\nu}^{\dagger} b_{\nu} + \frac{1}{4} \sum_{\nu_1, \nu_2, \nu_3, \nu_4} W_{\nu_1, \nu_2, \nu_3, \nu_4} b_{\nu_1}^{\dagger} b_{\nu_2}^{\dagger} b_{\nu_3} b_{\nu_4} - \sum_{\nu} (p_{\nu} b_{\nu} E + \text{H.c.}), \quad (3)$$

with the optical matrix element  $p_{\nu} = \int d^2r_e p_{\nu,c} \psi_{N,K}(\mathbf{r}_e, \mathbf{r}_e) \delta_{K,0}$ . Here  $p_{\nu,c}$  is the valence-conduction-band dipole matrix element. The first term gives the free  $X$  energies in the QWW. The second term describes the Coulombic  $X$ - $X$  interaction, and the last term describes the coupling of the  $X$ 's with the coherent light field. The matrix elements for the scattering of  $X$ 's with identical spin structure (e.g.,  $e\uparrow, h\downarrow$ ) are given by<sup>18</sup>

$$W_{\nu_1, \nu_2, \nu_3, \nu_4} = \int d^2r_{e1} \int d^2r_{e2} \int d^2r_{h1} \int d^2r_{h2} \times \psi_{\nu_1}(\mathbf{r}_{e1}, \mathbf{r}_{h1}) \psi_{\nu_2}(\mathbf{r}_{e2}, \mathbf{r}_{h2}) [V(\mathbf{r}_{e1} - \mathbf{r}_{e2}) + V(\mathbf{r}_{h1} - \mathbf{r}_{h2}) - V(\mathbf{r}_{e1} - \mathbf{r}_{h2}) - V(\mathbf{r}_{e2} - \mathbf{r}_{h1})] \times [\psi_{\nu_3}(\mathbf{r}_{e1}, \mathbf{r}_{h1}) \psi_{\nu_4}(\mathbf{r}_{e2}, \mathbf{r}_{h2}) + \psi_{\nu_3}(\mathbf{r}_{e2}, \mathbf{r}_{h2}) \psi_{\nu_4}(\mathbf{r}_{e1}, \mathbf{r}_{h1}) - \psi_{\nu_3}(\mathbf{r}_{e2}, \mathbf{r}_{h1}) \psi_{\nu_4}(\mathbf{r}_{e1}, \mathbf{r}_{h2}) - \psi_{\nu_3}(\mathbf{r}_{e1}, \mathbf{r}_{h2}) \psi_{\nu_4}(\mathbf{r}_{e2}, \mathbf{r}_{h1})], \quad (4)$$

where  $V(r) = e^2/\epsilon_0 r$ . Neglecting the dependence on the momentum transfer, one can show by a careful analysis that the direct Coulomb interactions [the first two terms in the last bracket of Eq. (4)] are of order  $\lambda^2$ , while the exchange interactions (last two terms) are of order  $\lambda$ , thus yielding the leading contributions. In the following, the direct interaction contributions and, as a consequence, interactions between  $X$ 's of different spin structures, are neglected. The exchange interaction yields in leading order

$$W_{\nu_1, \nu_2, \nu_3, \nu_4} = C_X \frac{a_B}{L_x} E_R \delta_{K_1+K_2, K_3+K_4} \alpha_{N_1, N_2, N_3, N_4}, \quad (5)$$

where  $E_R$  is the  $X$  Rydberg.  $C_X$  is a six-dimensional exchange integral, which has been evaluated numerically. The matrix elements  $\alpha$  describe the selection rules for the scattering between the various one-dimensional subbands:

$$\alpha_{N_1, N_2, N_3, N_4} = \frac{1}{8} (\delta_{N_1-N_2, N_3-N_4} + \delta_{N_1-N_2, -N_3+N_4} + \delta_{N_1+N_2, N_3+N_4} - \delta_{N_1-N_2, N_3+N_4} - \delta_{N_1-N_2, -N_3-N_4} - \delta_{N_1+N_2, N_3-N_4} - \delta_{N_1+N_2, -N_3+N_4}). \quad (6)$$

The phase relaxation time  $T_2$  can be derived, e.g., by diagrammatic perturbation theory. For the dephasing of  $X$ 's of subband  $N=1$ , one obtains

$$\begin{aligned} \frac{1}{T_2} = & -\frac{C_X^2 \lambda^2 \left(\frac{E_R}{k_B T}\right)^2}{8\pi} \sum_{N_1, N_2, N_3} \int_{-\infty}^{+\infty} dK \int_{-\infty}^{+\infty} dK' \\ & \times \alpha_{N=1, N_1, N_2, N_3}^2 [g_{N_2, K} g_{N_3, K'} (1 + g_{N_1, K+K'}) \\ & - (1 + g_{N_2, K})(1 + g_{N_3, K'}) g_{N_1, K+K'}] \\ & \times \delta_{\Gamma}(\epsilon_{N_2, K} + \epsilon_{N_3, K'} - \epsilon_{N_1, K+K'} - \epsilon_{N=1, 0}), \quad (7) \end{aligned}$$

where  $g_N(K)$  are the  $X$  distribution functions. The incoherent  $X$ 's generated by the prepulse are assumed to be in quasi-equilibrium with a temperature  $T$ . The common chemical potential of the thermal  $X$ 's is obtained from the excited  $X$  density.

In our theory, the influence of disorder on the DFWM signal of the QWW's is not included on a microscopic level. Several approaches for this influence have been reported,<sup>19</sup> which already show a high degree of complexity in the Hartree-Fock approximation. Instead, we use a phenomenological approach in which we calculate the dephasing time  $T_2$  by using the inhomogeneously broadened linewidth observed in the absorption spectra.

Nevertheless, in the present  $\text{In}_x\text{Ga}_{1-x}\text{As}/\text{GaAs}$  QWW's a significant part of the  $X$ 's is localized at low temperatures, as can be seen from the redshift of the luminescence lines in comparison to the excitation spectra (see Fig. 1). Fischer *et al.*<sup>20</sup> showed that the  $X$ - $X$  interaction rates for localized  $X$ 's are about one order of magnitude smaller than the interaction rates for free  $X$ 's. This reduction of the scattering rate can be attributed to the reduced spatial extension of the localized  $X$  wave function, giving these  $X$ 's a decreased scattering cross section. Thus, in a first approximation, the contribution of localized  $X$ 's to the homogeneous linewidth can be neglected, and it is mainly the free  $X$  scattering that determines the density dependence of  $\Gamma$ , as assumed in our theory. The best fit to the experimental data has been obtained, assuming that only about one-sixth of the generated  $X$ 's move freely with a temperature close to the bath temperature.

Equation (7) immediately provides the linear dependence of  $\Gamma$  on the  $X$  density, because the leading term of the products of distribution functions in the integral kernel is given by  $(1+g)(1+g)g \approx g$ . The inverse dephasing time is proportional to the square of the exchange interaction matrix elements, and therefore in lowest order proportional to  $\lambda^2$ . Thus,  $\gamma_{XX}$  is inversely proportional to the square of the wire width  $L_x$ , which explains the observed increase of  $\Gamma$  with decreasing  $L_x$ .<sup>21</sup>

The experimental results for  $\gamma_{XX}$ , as determined from linear fits of  $\Gamma$  versus  $n_X$ , are shown together with the the-

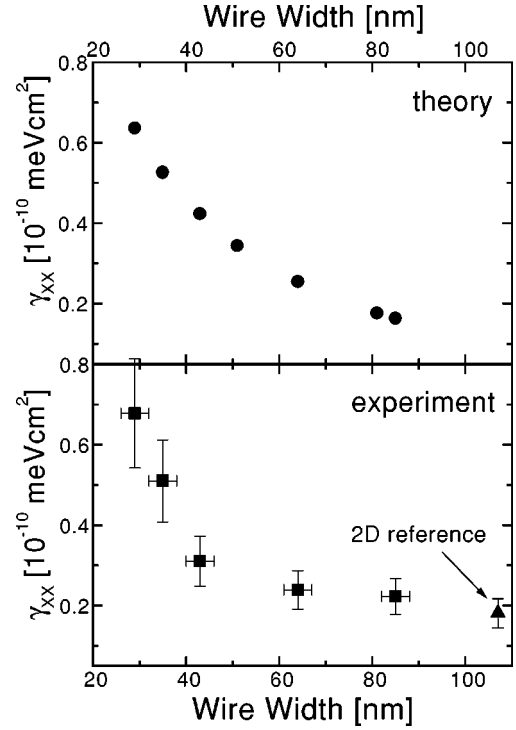


FIG. 5. Wire width dependence of the line broadening parameter  $\gamma_{XX}$ . The triangle gives the value of the quasi-two-dimensional reference. The upper part of the figure shows the theoretical results.

oretical results in Fig. 5. Experiment and theory are in excellent agreement for the dependence on the wire width  $L_x$ . For the two-dimensional reference we find a value of  $0.18 \times 10^{-10}$  meV cm<sup>2</sup>, which compares well with result of  $\gamma_{XX} = 0.12 \times 10^{-10}$  meV cm<sup>2</sup> published earlier.<sup>16</sup> For wires with sizes larger than about 50 nm, we obtain values for  $\gamma_{XX}$  comparable to that of the two-dimensional Ref. 22. For wires with widths below 50 nm, however,  $\gamma_{XX}$  increases drastically. In the case of 43-nm-wide QWW's,  $\gamma_{XX}$  is  $0.31 \times 10^{-10}$  meV cm<sup>2</sup>, and for 29-nm-wide wires  $\gamma_{XX}$  is already  $0.68 \times 10^{-10}$  meV cm<sup>2</sup>. This means that the  $X$ - $X$  scattering is more than three times as efficient in these small QWW's, in comparison to the two-dimensional reference.

In summary, we have investigated the  $X$ - $X$  scattering process in  $\text{In}_x\text{Ga}_{1-x}\text{As}/\text{GaAs}$  QWW's as a function of the lateral size. The parameter  $\gamma_{XX}$ , which is a measure of the  $X$ - $X$  scattering strength, increases strongly with decreasing wire width, as determined by DFWM experiments. A microscopic model for the  $X$ - $X$  scattering has been developed, which is in good agreement with the experimental findings.

The financial support by the Deutsche Forschungsgemeinschaft and by the Volkswagen Foundation is gratefully acknowledged.

- <sup>1</sup>H. Benisty, C. M. Sotomayor-Torrès, and C. Weisbuch, *Phys. Rev. B* **44**, 10 945 (1991).
- <sup>2</sup>H. Sakaki, *Jpn. J. Appl. Phys.* **19**, L735 (1980).
- <sup>3</sup>M. Preisel, J. Mørk, and H. Haug, *Phys. Rev. B* **49**, 14 478 (1994).
- <sup>4</sup>M. Kohl, D. Heitmann, P. Grambow, and K. Ploog, *Phys. Rev. Lett.* **63**, 2124 (1989).
- <sup>5</sup>Y. Nagamune, Y. Arakawa, S. Tsukamoto, M. Nishioka, S. Sasaki, and N. Miura, *Phys. Rev. Lett.* **69**, 2963 (1992).
- <sup>6</sup>R. Rinaldi, R. Cingolani, M. Lepore, M. Ferrara, I. M. Catalano, F. Rossi, L. Rota, E. Molinari, P. Lugli, U. Marti, D. Martin, F. Morier-Gemoud, P. Ruterana, and F. K. Reinhart, *Phys. Rev. Lett.* **73**, 2899 (1994).
- <sup>7</sup>T. Someya, H. Akiyama, and H. Sakaki, *Phys. Rev. Lett.* **76**, 2965 (1996).
- <sup>8</sup>F. Rossi, G. Goldoni, and E. Molinari, *Phys. Rev. Lett.* **78**, 3527 (1997).
- <sup>9</sup>S. Rudin, T. L. Reinecke, and B. Segall, *Phys. Rev. B* **42**, 11 218 (1990).
- <sup>10</sup>M. Oestreich, W. W. Rühle, H. Lage, D. Heitmann, and K. Ploog, *Phys. Rev. Lett.* **70**, 1682 (1993).
- <sup>11</sup>E. J. Mayer, J. O. White, G. O. Smith, H. Lage, D. Heitmann, K. Ploog, and J. Kuhl, *Phys. Rev. B* **49**, 2993 (1994).
- <sup>12</sup>W. Braun, M. Bayer, A. Forchel, H. Zull, J. P. Reithmaier, A. I. Filin, S. N. Walck, and T. L. Reinecke, *Phys. Rev. B* **55**, 9290 (1997).
- <sup>13</sup>J. Kuhl, A. Honold, L. Schultheis, and C. W. Tu, *Festkörperprobleme* **29**, 157 (1989).
- <sup>14</sup>T. Yajima and Y. Taira, *J. Phys. Soc. Jpn.* **47**, 1620 (1979).
- <sup>15</sup>For the determination of the  $X$  density, we assume that each absorbed photon generates an  $e$ - $h$  pair. Further, the time delay of 40 ps between the prepulse and the FWM pulses is clearly smaller than  $T_1$ , so that recombination processes are negligible. The number of absorbed photons is calculated by multiplying the number of photons in the prepulse (as determined from the laser pulse power) with the absorption of the pulse which has been normalized by the laser transmission spectrum after removing the sample.
- <sup>16</sup>A. Honold, L. Schultheis, J. Kuhl, and C. W. Tu, *Phys. Rev. B* **40**, 6442 (1989).
- <sup>17</sup>D. S. Kim, J. Shah, J. E. Cunningham, T. C. Damen, W. Schäfer, M. Hartmann, and S. Schmitt-Rink, *Phys. Rev. Lett.* **68**, 1006 (1992).
- <sup>18</sup>H. Haug and S. Schmitt-Rink, *Prog. Quantum Electron.* **9**, 3 (1984).
- <sup>19</sup>See, e.g., C. Lonsky, P. Thomas, and A. Weller, *Phys. Rev. Lett.* **63**, 652 (1989); R. Zimmermann, *Phys. Status Solidi B* **173**, 129 (1992); F. Jahnke, M. Koch, T. Meier, J. Feldmann, W. Schäfer, P. Thomas, S. W. Koch, E. O. Göbel, and H. Nickel, *Phys. Rev. B* **50**, 8114 (1994); R. Zimmermann, E. Runge, and F. Grosse, in *Proceedings of the 23rd ICPS, Berlin*, edited by M. Scheffler and R. Zimmermann (World Scientific, Singapore, 1996), p. 1935.
- <sup>20</sup>A. J. Fischer, D. S. Kim, J. Hays, W. Shan, J. J. Song, D. B. Eason, J. Ren, J. F. Schetzina, H. Luo, and J. K. Furdyna, *Phys. Rev. B* **50**, 17 643 (1994).
- <sup>21</sup>More accurately, the calculated  $\lambda$  dependence of  $\Gamma$  can be fitted with a cubic polynomial  $a\lambda^2 + b\lambda^3$ .
- <sup>22</sup>The value of  $\gamma_{XX} = 0.24 \times 10^{-10}$  meV cm<sup>2</sup> for our 64-nm-wide QWW's compares well with the value of about  $0.2 \times 10^{-10}$  meV cm<sup>2</sup> Mayer *et al.* (Ref. 11) obtained for their 60-nm-wide QWW's.